DEVELOPMENT OF MEMS ANGULAR RATE SENSOR FOR HIGH-DYNAMICS APPLICATIONS

Woon-Tahk Sung[*], Jang Gyu Lee[*], Taesam Kang[**], and Hyun-Gee Jang[***]

[*] *School of Electrical Engineering and Computer Science, Seoul National University, Seoul, 151-744, Korea*
[**] *School of Aerospace Engineering, Konkuk University, Seoul, 143-701, Korea*
[***] *IntelliMicrons, 8F Hansin IT tower II, 60-18 Gasan-dong, Geumcheon-gu, Seoul, 153-801, Korea*

Abstract: In this paper, presented are a design and test results of MEMS angular rate sensor of wide input range and wide bandwidth. Open loop performances of conventional MEMS rate sensor are very limited because of its nonlinear input-output relationship and very small bandwidth. In this study, a phase lead control scheme is applied to enlarge the operating range of the sensor. The structure of angular rate sensor is fabricated using MEMS manufacturing process and the detection circuit is designed applying the control circuit. From the test results, it is confirmed that the designed sensor has wide input range up to 1,000 deg/sec and bandwidth of 80 Hz.

Keywords: Analog control, Angular velocity, Closed-loop control, Inertial sensors, Gyroscopes.

1. INTRODUCTION

Great advances in micro-electromechanical systems (MEMS) technologies enable researchers to develop smaller and lighter sensors that are more applicable to various areas. MEMS gyroscope is an inertial sensor that is one of most widely studied sensors in these days adopting such a technology. It has various good properties such as low power consuming, very rigid, and easy to be fabricated cheaply by mass-producing process. It can provide not only the conventional application such as INS (inertial navigation system), but various new applications in the consumer industry (Yazdi, *et al*., 1998). Although the MEMS gyroscope offers good prospects of future inertial sensors, it needs more performance enhancement if it is to be applied to high-dynamics applications, i.e. wide input-range and wide bandwidth. In order to achieve wide input range and bandwidth, the sensor should offer linear output to wide range of angular rate input and the linearity should be maintained.

Since the conventional operating principle of the capacitive-sense MEMS gyroscope is based on the oscillating motion of a high-Q system, its bandwidth is very limited (Sung, *et al*., 2002). A system of small bandwidth has a small gain at high frequency input, which means it fails to follow a rapidly changing input.

In order to overcome such a limitation, it is considered that the displacement of the mass should be maintained under some restricted level even in a large input. In that case, however, the sensitivity to the input is also limited, which is not a desirable property of the sensor. In this paper, a feedback control scheme is adopted in a detection circuit as an effective solution for good performances. Feedback controller enables us to achieve a wide input range and a wide bandwidth without sacrificing the sensitivity of the sensor (Sung, *et al*., 2002). In this paper, several features of MEMS angular rate sensor and a feedback control scheme are illustrated and circuit implementation and experiments are accomplished to verify the performance of manufactured circuit.

2. SYSTEM ILLUSTRATION

2.1 Principle of operation

Fig. 1 illustrates the basic operational principle of MEMS angular rate sensor. The proof mass is driven along the driving axis (y-axis) at the resonant

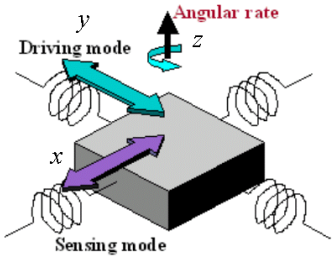

Fig. 1. The operational principle of MEMS angular rate sensor

frequency of the driving mode by sinusoidal driving voltage signal. When an angular rate input along *z*-axis is applied to the sensor, the oscillation of the mass along the sensing axis (*x*-axis) is induced, which is modulated by the vibration along the driving axis. The input angular rate is measured by detecting the capacitance change. Therefore the mechanical sensitivity to the rate input is basically influenced by those two modes of the gyroscope (He and Najafi, 2002; Lim, *et al*., 2002; Song, *et al*., 2001; Sung, *et al*., 2002; Seshia, *et al*. 2002).

The governing equations of MEMS gyroscope can be expressed as equations (1)-(6). When the proof mass is driven by the electrostatic force or $F_{driving}$(t) along the driving axis, the equation of the dynamic motion of the mass can be simply expressed as a second order mass-damper-spring system,

$$M_y\ddot{y}(t) + C_y\dot{y}(t) + K_y y(t) = F_{driving}(t) \qquad (1)$$

where M_y is the mass of the moving plate, C_y, the damping coefficient of the air-damper, K_y the spring constant along the driving axis. Then the transfer function from the driving force to the displacement of the plate is given by

$$G_{drive}(s) = \frac{Y(s)}{F_{driving}(s)} = \frac{1/M_y}{s^2 + \frac{C_y}{M_y}s + \frac{K_y}{M_y}}. \qquad (2)$$

If the angular rate input Ω_z(t) is applied along z-axis, *Coriolis* force is induced, which is given by

$$F_{Coriolis}(t) = 2M_y\dot{y}(t)\Omega_z(t). \qquad (3)$$

And the dynamic equation and the transfer function of the sensing mode can be expressed as (4) and (5), respectively.

$$M_x\ddot{x}(t) + C_x\dot{x}(t) + K_x x(t) = F_{Corilois}(t) \qquad (4)$$

$$G_{sense}(s) = \frac{X(s)}{F_{Coriolis}(s)} = \frac{1/M_x}{s^2 + \frac{C_x}{M_x}s + \frac{K_x}{M_x}} \qquad (5)$$

2.2 Input-output nonlinearity

Since the angular rate input, which produces *Coriolis* force, is measured by detecting capacitive change between the proof mass and sensing electrodes as illustrated in the previous section, the measurement of the rate is is basically nonlinear. If a parallel-capacitor-type sensing scheme is used in a sensor development, relatively large nonlinearity is inevitable compared with piezo-type sensing (Yang, *et al*. 2002). In order to overcome such a problem, a differential-type sensing scheme is widely used (Lim, *et al*., 2002; Luo, *et al*., 2002; Song, *et al*., 2001; Sung, *et al*., 2002) as shown in Fig. 2. Using such a configuration, the sensitivity to the input is doubled and the input-output linearity is improved, which is shown in Fig. 3. Corresponding equation is expressed in (6), where N denotes number of electrodes pair, ε is electrical permittivity, and A is area of electrode plate. If the displacement of the mass due to the *Coriolis* force is restricted around the zero-input region, a linear relation is guaranteed within some desired level. However, if the displacement goes over certain limited range, nonlinearity is dramatically increased as shown in the figure.

$$\begin{aligned}\Delta C = N(C_1 - C_2) &= N\left(\varepsilon\frac{A}{x_0 - x} - \varepsilon\frac{A}{x_0 + x}\right) \\ &= \frac{N\varepsilon A}{x_0}\left(\frac{1}{1 - x/x_0} - \frac{1}{1 + x/x_0}\right)\end{aligned} \qquad (6)$$

If more linear relationship is needed in wider range of input, comb-type sensing scheme could be one of the solutions. Fig. 4 depicts the concept of the comb-type capacitive sensing scheme. From the design, linear relation is well achieved since the capacitance

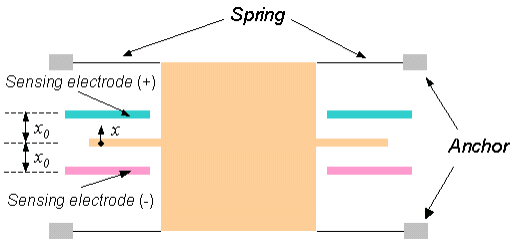

Fig. 2. Differential-parallel-type sensing scheme of MEMS gyroscope

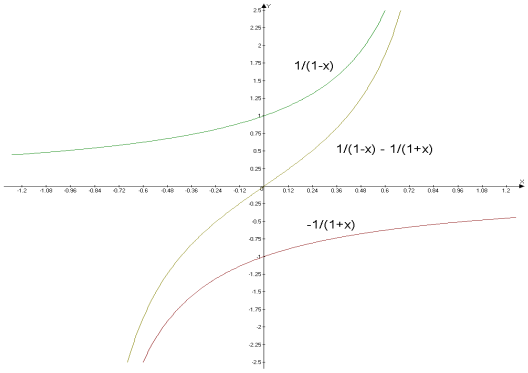

Fig. 3. Input-output relation of capacitance change of differential-parallel-type sensing scheme

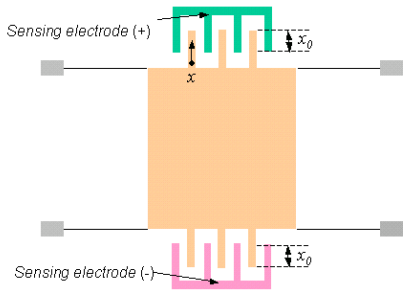

Fig. 4. Comb-type sensing scheme of MEMS gyroscope

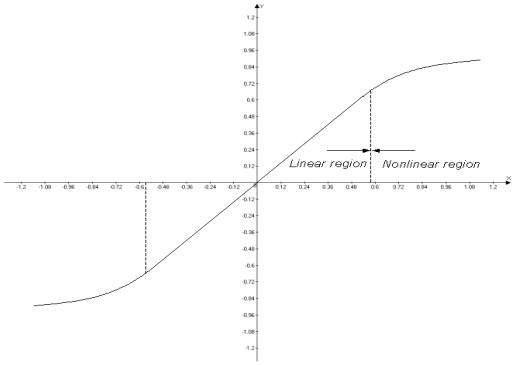

Fig. 5. Nonlinear output of comb-type sensor

between mass and electrodes are directly proportional to the displacement of the mass if a fringing effect is neglected. The linearity is guaranteed if the stiffness of the plate spring is ideally constant up to large inputs, which is not true in real sensors. If the range of the input goes over certain bounded level, the displacement of the mass is rapidly reduced as shown in Fig. 5. Moreover, the large input can destroy the spring suspension. Therefore, the operating range should be restricted within the linear region. If the input range of sensor is desired to be very large, the spring stiffness must be increased to reduce the displacement of the proof mass. That case, however, leads to a low sensitivity to the rate input, which is not desirable.

2.3 Small bandwidth: high-Q system

The operation of the MEMS gyroscope, as illustrated in previous section, is based on the oscillating movement of the mass at the resonant frequency of the spring-mass-damper system. The operating

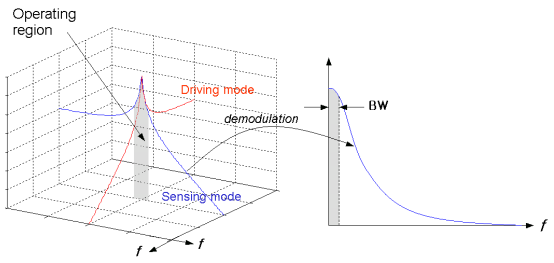

Fig. 6. Frequency response plot of two modes and demodulated output of sensing mode

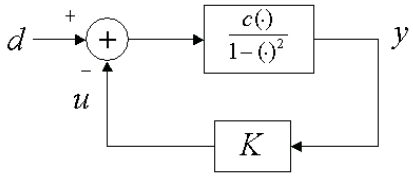

Fig. 7. Block diagram of feedback control in nonlinear plant of capacitive sensing scheme

region is an overlapped area of resonant frequency regions of two orthogonal driving and sensing part dynamics (here after, it is called as a 'mode'), which is illustrated in Fig. 6. Frequency response plot of the sensor is shown in the right side of the figure, which is a demodulated output of the sensing mode (Sung, *et al*., 2002). Since the operating region is in a high-Q mode, bandwidth of the output is very limited as shown in the figure. This means the system cannot follow the high frequency input (or rapidly changing input). In order to achieve wider bandwidth, a low-Q system could be considered by designing the structure operating in high damping atmosphere. But, in that case, similar to the previous case of high spring stiffness, the sensitivity to input also decreases.

3. CONTROL CIRCUIT DESIGN

3.1 Nonlinearity error: proportional control

Considering the differential capacitive sensing scheme in section 2.1, the output of the sensor can be expressed in terms of the capacitance calculation equation as in (7), where $c = 2c_0\varepsilon A / x_0$ denotes a coefficient gain of the detection circuit including various circuit gain at each stages and $d = x / x_0$ is a normalized displacement of the proof mass.

$$y = c_0\left(\frac{N\varepsilon A}{x_0 - x} - \frac{N\varepsilon A}{x_0 + x}\right) = \frac{2c_0\varepsilon A / x_0 \cdot (x / x_0)}{1 - (x / x_0)^2} = \frac{c \cdot d}{1 - d^2} \quad (7)$$

Eq. (7) is clearly nonlinear one whose output rapidly increases as $d = x / x_0$ goes 1 (or x goes x_0). If a

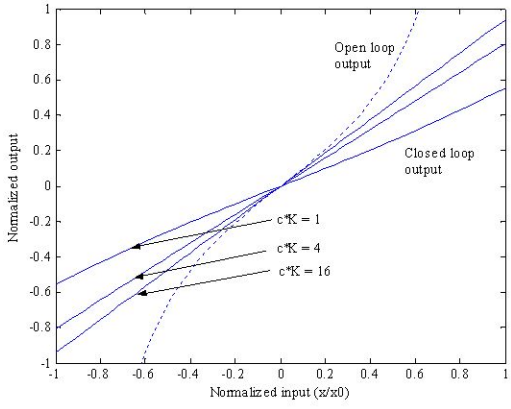

Fig. 8. Open and closed loops output plot of parallel type capacitive sensing

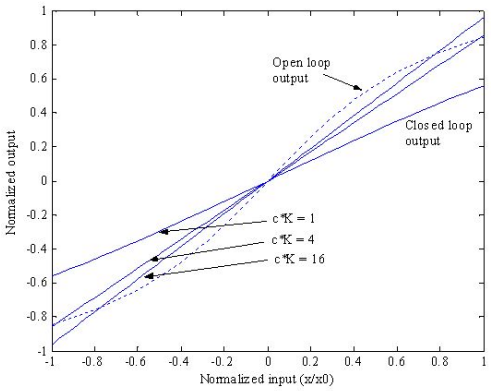

Fig. 9. Open and closed loops output plot of comb type capacitive sensing with saturation property

feedback control is applied as shown in Fig. 7, then (8) holds. Elimination of variable y leads the nonlinear relation between normalized displacement d and controller output u as shown in (9).

$$y = \frac{c \cdot (d-u)}{1-(d-u)^2}, \; u = Ky \tag{8}$$

$$u^3 - 2du^2 + (d^2 - cK - 1)u + cKd = 0 \tag{9}$$

From the equation, a graph of u versus d can be plotted as shown in Fig. 8. The graph shows that the output of the closed loop is almost straight comparing with that of the open loop output shown as a dotted line in the figure. Table 1 lists the nonlinearity errors of two systems when the displacement ratio is half of full range, i.e. $d = 0.5$.

Table 1 Nonlinearity errors of open and closed loop in Fig. 8

		Nonliearity error
Open loop		6.4%
Closed loop	c*K = 1	0.58%
	c*K = 4	0.039%
	c*K = 16	0.001%

The data shows that the nonlinearity error is dramatically reduced by the control. As a matter of fact, the input range can be enlarged up to almost infinity range by applying controller if the operating range of the circuit components supports it.

In case of comb-type capacitance sensing, the linearity improvement through feedback control is also guaranteed, which is depicted in Fig. 9. The nonlinearity error of controlled output is almost same as listed in Table 1. In fact, all kind of nonlinearities in open loop systems can be reduced by control since the output is no more dependent to the plant but directly follows the input.

3.2 Stability: derivative control

In previous section, as the control gain increases, the linearity of the system is improved. The stability in

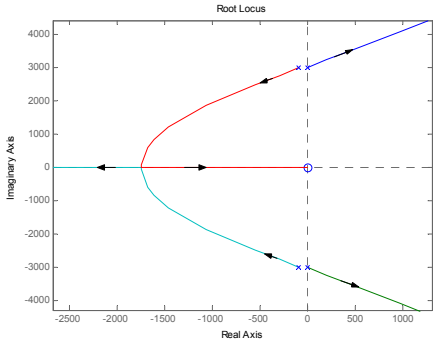

Fig. 10. Root locus of the proportional controller

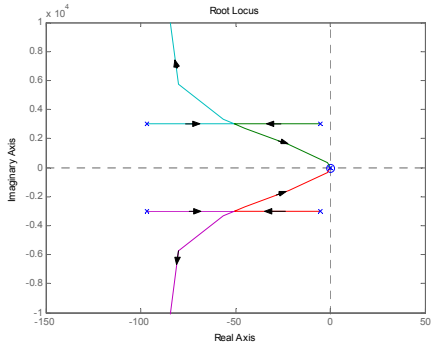

Fig. 11. Root locus of the derivative controller

the feedback system, however, is not directly achieved if the proportional gain control is only used, which is illustrated in Fig. 10. The plant consists of two transfer function blocks, i.e. sensing mode dynamics of second order mass-damper-spring system and band-pass filter that is used in signal conditioning for effective signal process. Therefore, four poles and one zero are shown in the figure, which leads unstable system if the feedback gain increases. If another zero near the origin is inserted, the system can be stabilized at any condition, which is realized by phase lead compensator or PD control. In this case, since the operating point of the sensor is high-frequency region, integral control does little role in the feedback system.

3.3 Bandwidth

In addition to the linearity improvement, the

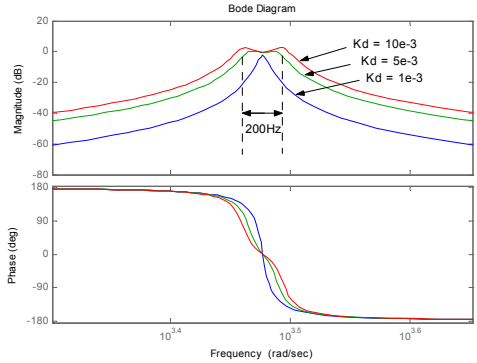

Fig. 12. Frequency response plot of controller output when the derivative gain varies

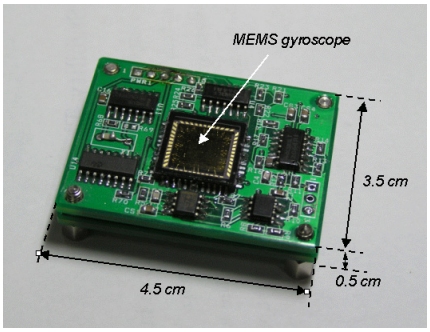

Fig. 13. Fabricated detection and control circuit

bandwidth of the system can be improved by the feedback control. In previous section, the stability of the feedback system can be achieved by inserting a derivative gain control. Moreover, adjusting derivative gain can give enlarged bandwidth of the system. Fig. 12 shows that the output of the controlled system in a frequency domain as the derivative control gain is adjusted. If the derivative control gain or K_d is increased, the bandwidth of the system is widened and the tracking ratio to the input is increased (amplitude of the peak point goes near to 0 dB point). 200Hz bandwidth is marked in the figure. Since the final output is obtained by demodulating the controller output signal, actual bandwidth is reduced to a half (100 Hz) for that case. In the figure, if the gain is increased for the bandwidth of more than 200 Hz, the peak area is distorted, which leads an overshoot of output signal. Therefore the gain should be properly adjusted to have enough bandwidth without a large overshoot.

3.4 Circuit implementation

Accomplished is the circuit implementation of control system of MEMS gyroscope. First of all, signal processing parts including driving, capacitive detection and demodulation circuit are designed and tested in printed circuit board. Then the control circuit is inserted and tested. The sample chip of MEMS gyroscope is mounted on the circuit. Fig. 13 shows the fabricated gyroscope and circuit. Driving frequency of the sensor is 7 kHz, which is the resonant frequency of the sensing mode and a carrier is used for effective signal processing which is a 110 kHz sinusoidal signal. PD controller is realized using a couple of resistors, capacitors and op-amps. Using the designed circuit, following experiments are accomplished.

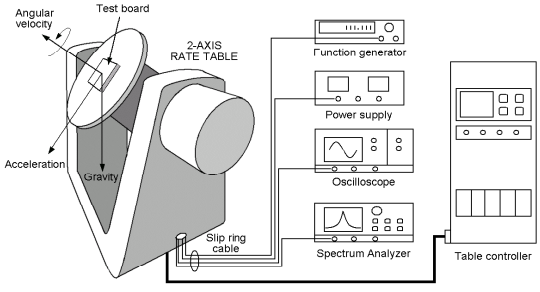

Fig. 14. Experimental setup

4. EXPERIMENTS

The experimental setup is shown in Fig. 14. Angular rate signal is generated using a rate table for low frequency input, and a rate equivalent voltage signal is used for the high frequency input and extremely large rate input using a function generator. Output signal is measured by test equipment through the slip ring cable.

At first, nonlinearity test was accomplished, which is shown in Fig. 15 and 16. Angular rate input of 1,000 deg/sec is applied to the sensor and output signal is measured in time domain compared with the reference input signal that is provided by the table controller. Fig. 15 shows that the open loop output, in which nonlinear behaviour is observed when the magnitude of input increases. Nonlinearity error of the open loop is about 6% that is undesirable performance of the sensor. On the other hand, the nonlinearity error of controlled system is reduced to 0.5%, which is shown in Fig. 16. If the control gain is increased, the nonlinearity error can be decreased less than 0.5%. In that case, however, noise in the circuit is somewhat increased, and it is not easy to distinguish such a small nonlinearity due to the noise.

Bandwidth tests are performed by applying a step input using a function generator, which is a virtual input equivalent to angular rate. The test results are shown in Fig. 17 and 18. If the rising time is measured, the bandwidth of the system can be calculated. From the results, bandwidth of the closed

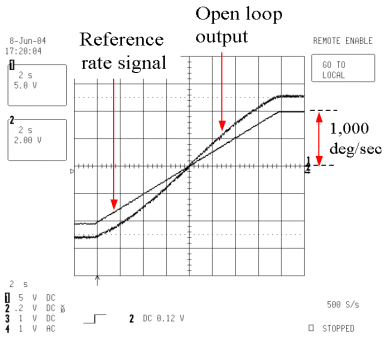

Fig. 15. Linearity test: Open loop

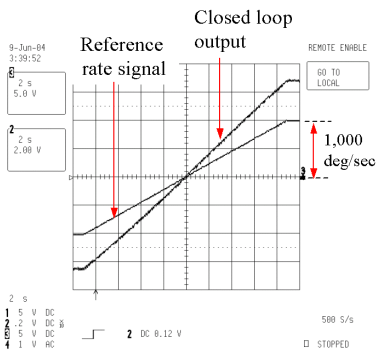

Fig. 16. Linearity test: Closed loop

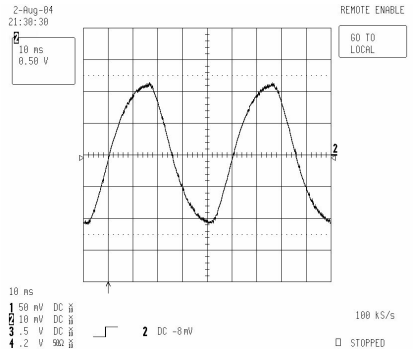

Fig. 17. Output of open loop system to the square angular rate input

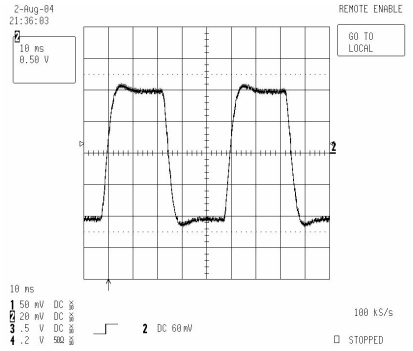

Fig. 18. Output of open loop system to the square angular rate input

loop system is up to 80 Hz, whereas the original system of open loop gives around 10 Hz bandwidth. The closed loop bandwidth can be increased more if the control gain is increased. In that case, however, the big overshoot occurs and the noise in the circuit is likely to increase, which can lead the system unstable.

5. CONCLUSIONS

In this study, a MEMS angular rate sensor of wide input range of 1,000 deg/sec and bandwidth of 80 Hz is developed and tested. The MEMS sensor is a very small sized one and has many applications in the future market. But due to the inherent property of its nonlinear detection scheme and high-Q system, it needs new detection scheme if it is to be applied to the high-dynamics applications.

In this study, feedback control circuit is applied to achieve such a goal. Feedback controller enables us to have high linearity and wide bandwidth without sacrificing the sensitivity of the sensor. Since the operating point of the sensor is high frequency region, a phase lead control scheme is used. From the test results, it is verified that the designed controller improve the performance of the sensor compared with the open loop results.

ACKNOWLEDGMENT

The authors would like to thank for the support of ASRI and BK-21 project in Seoul National University, Korea, the Korea Research Foundation Grant (KRF-2004 -0055- B00047), and Aerospace Technology Development Project.

REFERENCES

He, G., and K. Najafi (2002), A Single-Crystal Silicon Vibrating Ring Gyroscope, Technical Digest, IEEE 2002 Int. Conference on Micro Electro Mechanical Systems (MEMS 2002), Las Vegas.

Lim, Hyung-Taek, Jin-Woo Song, Jang-Gyu Lee and Yong-Kweon Kim (2002), Few deg/hr resolvable low noise lateral microgyroscope, IEEE MEMS Conference, Las Vegas, NV, pp. 627-630

Luo, H., LR Carley and GK Fedder (2002), Copper CMOS-MEMS Z-Axis Gyroscope, IEEE MEMS Conference, Las Vegas, NV, pp. 631-634.

Seshia, A. A., R. T. Howe, and S. Montague (2002), An integrated microelectromechanical resonant-output gyroscope, 15th IEEE Micro Electro Mechanical Systems Conference (MEMS 2002), Las Vegas, Nevada.

Song, J.W., J.G. Lee, T. Kang, W.T. Sung, H.T. Lim, and Y.K Kim (2001), Design of a Gimbal-Structured Micro Gyroscope and Signal Processing Part, Proceedings of ICCAS2001, pp.1266-1269.

Sung, Woon-Tahk, Jin Woo Song, Sangkyung Sung, Jang Gyu Lee and Taesam Kang (2002), Feedback loop design for micro gyroscope, Proceedings of ICCAS2002, pp. 234-238.

Yang, H., M. Bao, H. Yin, S. Shen (2002), A novel bulk micromachined gyroscope based on a rectangular beam-mass structure, *Sens Actuators* A96, pp. 145-151.

Yazdi, N., F. Ayazi and K. Najafi (1998), Micromachined Inertial Sensors Proceeding of the IEEE, vol. 86, No. 8, pp. 1640-1659.